

Morphology of Silver Particulate Films Deposited on Softened Polymer Blends of Polystyrene and Poly (4-vinylpyridine)

Pratima Parashar

Department of Materials Science, Mangalore University, Mangalagangothri 574199, India

Received 13 May 2010; accepted 10 October 2010

DOI 10.1002/app.33590

Published online 24 February 2011 in Wiley Online Library (wileyonlinelibrary.com).

ABSTRACT: Results of the morphological studies of silver particulate films deposited at a rate of 0.4 nm/s on polymeric blends of polystyrene (PS) and poly (4-vinylpyridine) (P4VP) held at a temperature 457 K by evaporation in a vacuum of 8×10^{-6} Torr are reported here. The morphology of silver particulate films was characterized by their size, size distribution, shape and interparticle separation. It has been observed that morphology depends on the composition of polymer matrix and the amount of silver deposited. The red shift in the plasmon resonance was observed with the increasing amount of P4VP in the blends in comparison to the pure PS. This indicates the

modification in the silver particulate films deposited on the PS/P4VP blends. Scanning electron microscopy (SEM) was used to study the change in morphology of the silver nanoparticles and was correlated with the optical properties of silver particulate films on PS/P4VP blends. The silver nanoparticles deposited on the thin layers of polymer blends exhibit smaller size with narrower dispersion and wider size distribution due to blending of P4VP with PS. © 2011 Wiley Periodicals, Inc. *J Appl Polym Sci* 121: 839–845, 2011

Key words: nanoparticles; polymer blends; thin films; vapor deposition; optical properties

INTRODUCTION

Silver nanoparticles embedded in polymer matrices are a broad area of research because of their unique structural, optical, electronic and electrical properties.^{1–6} These have attracted particular interest due to their favorable optical properties, displaying surface plasma resonance.⁷ Polymer matrices have been frequently used as particle stabilizers in chemical synthesis of metal colloids since these prevent agglomeration of the particles.⁸ Polymeric matrix provides the ability of processing and flexibility. This is the unique possibility of controlling viscosity of the softened polymer substrate and hence the structural properties of the silver particulate films deposited on polymer blends.

Nanocomposites of metal nanoparticles in a polymer matrix have generated a great deal of interest which depends on the metal-polymer composition and their structure. Polymers are particularly attractive as the dielectric matrix in composites due to their versatile nature and can easily be processed into thin films. These nanocomposites exhibit a unique combi-

nation of desirable optical and electrical properties that are otherwise unattainable.^{9–13} All these properties depend on the size, size distribution and shape of the nanoparticles. The growth and arrangement of metal nanoparticles on various substrates are therefore key issues in all the fields of modern science and technology relating to nanoelectronics, photonics, catalysis, and sensors.¹⁴ The ability to tailor and optimize the nanocomposite structure precisely creates opportunities for a wide range of applications.

Metal-polymer nanocomposite containing widely separated nanoparticles exhibit insulating behavior. As the percentage of metal in composite increases, the nanoparticles separation decreases. At a certain thickness of silver on softened polymer substrate, nanoparticles are quite densely packed but separated by polymer gap such a film offer a host of unique property relevant to practical applications. These applications include high dielectric constant passives, electromagnetic interference shielding, sensors, and detector designed for a variety of specific purposes with high performances, sensitivity, and flexibility.¹⁵ Further, the morphology of the cluster films deposited on softened polymer substrates is dependent on the polymer-metal interaction. Gold deposited on polystyrene and subsequently annealed above its glass transition temperature results in a highly agglomerated film with large separation between the clusters, possibly due to inert nature of PS.¹

Correspondence to: P. Parashar (pratimaparashara@rediffmail.com).

Contract grant sponsor: Women Scientist Scheme (WOS).

Silver deposited on polystyrene also forms highly agglomerated subsurface particulate structure with large separations between the metal particles.¹⁶ But, silver deposited on an interacting polymer like poly (4-vinylpyridine) resulted in the formation of smaller particles (approximately a few tens of nm) with smaller interparticle separations.¹⁷ The differences in dispersion, size distribution, and impregnation depth result from the differing natures of the polymer hosts and the processing conditions.¹⁸ Therefore, it is interesting to restrict the nanoparticles to a small size regime along with a narrow size distribution by blending inert PS with interacting P4VP.

Our previous work,¹⁹ electrical behavior of silver particulate films on PS/P4VP blends show subsurface formation of films resulted in room temperature resistance in the range desirable for device applications. But silver deposited on softened inert polymer like polystyrene substrates show room temperature resistances equalling that of the substrate, irrespective of the thickness deposited because of highly agglomerated structures. This suggests the possibility of modification in morphology of silver particulate films on PS/P4VP blends. Polymer blending is a common way to develop new polymer materials with desirable combinations of properties. The main advantage of this method is to control the properties by varying the blend compositions.⁸

In this article, we have discussed the morphology of silver particulate films on PS/P4VP blends.

EXPERIMENTAL

Poly (4-vinylpyridine) and silver (purity better than 99.99+%) used in this study were procured from Sigma-Aldrich Chemicals Pvt. Ltd. Polystyrene was procured from Alfa-Aesar (A Johnson Mathley Company). The average molecular weight of P4VP and PS are 60,000 and 100,000, respectively. Polymer blends were prepared through solution blending by mixing in a common solvent, diethylformamide (DMF). Blends of PS/P4VP with different compositions {PS (w)/P4VP (w) = 0 : 100; 25 : 75; 50 : 50; 75 : 25; 100 : 0} were prepared. About 2 g of the total polymers at different ratios were dissolved in 20 mL of DMF at room temperature. Silver films of various thicknesses were vacuum evaporated onto softened polymer blends of PS/P4VP, solution cast on glass substrates held at temperature of 457 K, above the glass transition temperatures of homopolymers in a vacuum better than 8×10^{-6} Torr at a rate of 0.4 nm/s. A chromel-alumel thermocouple was used to measure the substrate temperature by clamping it to the substrate surface holding the film. Source to substrate distance was maintained at 20 cm. A Telemark quartz crystal monitor (Model 850) was

used to measure the deposition rate, as well as the overall film thickness. Optical absorption spectra of the silver particulate films were obtained on a Shimadzu UV-Vis-NIR spectrophotometer model SHIMADZU UV 3101 PC. X-ray diffraction (XRD) studies were carried out for particle size measurements with the diffraction angle 2θ equal to 38° using a BRUKER D8 ADVANCE powder x-ray diffractometer with Cu-K α radiation. Scanning electron microscopy (SEM) measurements were carried out on a Leica Cambridge Instruments Stereo scan 440 SEM with image processing software. The acceleration voltage is 20 kV and magnification is 50–100 KX.

RESULTS AND DISCUSSION

Optical studies

Figure 1(a) shows the optical absorption spectra recorded for 50 nm silver films deposited on polymeric blends held at 457 K at the deposition rate of 0.4 nm/s. It is well known that small silver particles embedded in polymer matrix exhibit plasmon resonance absorption and as a result absorption maxima occur in the visible-near infrared region and their spectral position depends on the particle size, shape, filling factor etc. in the polymer matrix. The surface plasmon resonance absorption for silver clusters in the polymer matrix generally occurs at a wavelength of ~ 430 nm.¹⁷ It is well known that shift in the plasmon resonance peak towards higher wavelength occurs due to close proximity of the silver clusters.^{20–23} These nanoparticles exhibit unique optical properties originating from the characteristic surface plasmon by the collective motion of conduction electrons.^{22,23}

Thus, the formation of silver nanoparticles can also be confirmed by UV/VIS absorption spectrum of composite films.²⁴ Spectral position, half width and intensity of the plasmon resonance strongly depend on the particle size, shape, and the dielectric properties of the particle material and the surrounding medium.²⁵ The type of metal and the surrounding dielectric medium play a significant role in the excitation of particle plasmon resonance (PPR). The sensitivity of PPR frequency to small variations of these parameters can be exploited in various applications.²⁶ For silver particles embedded in PS/P4VP blends, a shift of the resonance position to higher wavelength (red shift) were found, which were correlated with changes of particle sizes and inter-separation in the silver clusters. It is clearly seen [Fig. 1(a)] that the plasmon resonance peak shifts towards the longer wavelength side in comparison to pure PS (485.5 nm). It is 598, 651.6, and 754.5 nm for PS : P4VP, 75 : 25, 50 : 50, and 25 : 75, respectively, for 50 nm silver particulate film on them.

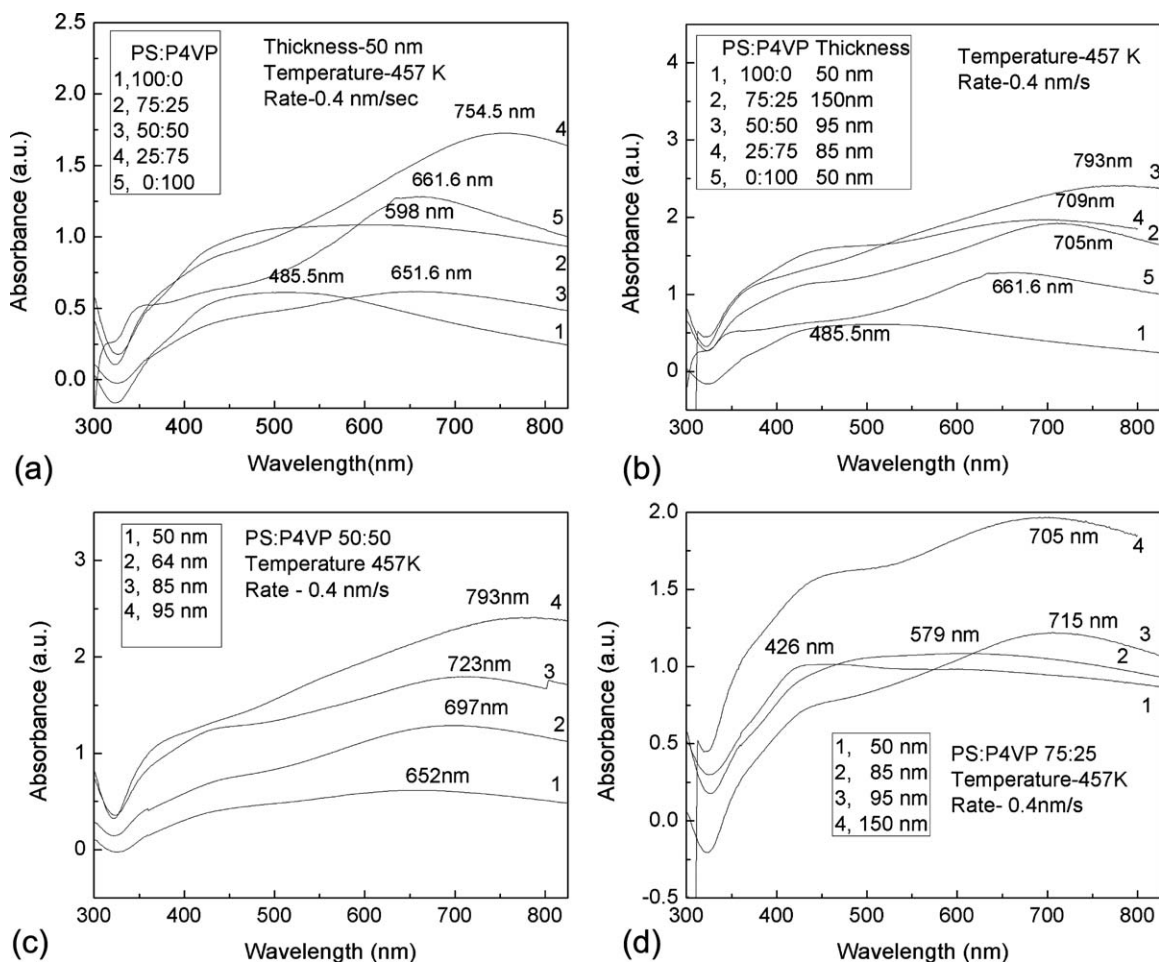


Figure 1 (a) Optical absorption spectra for 50 nm silver particulate films deposited on PS/P4VP blends. (b) Optical absorption spectra for the films of various thicknesses deposited on the PS /P4VP blends. (c) Optical absorption spectra for the films deposited on the blend PS/P4VP 50 : 50. (d) Optical absorption spectra for the film deposited on the blend PS/P4VP 75 : 25.

Also, there is increase in intensity of absorbing peaks which can be attributed to the decrease of particles size with the incorporation of P4VP into PS.²⁴

Previous studies²⁷ of silver particulate film on PS for the 50 nm thickness exhibited minimum shift due to the presence of comparatively larger clusters with larger intercluster separations than on P4VP²⁸ for the same thickness. Blending of P4VP with PS is expected to provide a polymer matrix where the size of silver clusters and intercluster separation can be modified because dispersion, size distribution and impregnation depth results from the natures of polymeric hosts.⁶

Figure 2(c) shows the XRD pattern with the diffraction peak around 38° for the silver particulate films of thickness of 50 nm on P4VP, PS and PS/P4VP, 25 : 75, 50 : 50, and 75 : 25. The broadening of the Bragg peaks indicates the formation nanoparticles. The particle sizes calculated from the Figure 2(c) are 53, 51, 49, 46, and 30 nm for the blends (PS : P4VP) 100 : 0, 75 : 25, 50 : 50, 25 : 75,

and 0 : 100, in that order. The particle sizes estimated from XRD suggest that there is a very small reduction in particle size due to blending of PS and P4VP. Figure 2(d) shows the XRD patterns for the silver particulate films on PS/P4VP, 75 : 25, 50 : 50 and 25 : 75 for 150, 95, and 85 nm thicknesses, respectively. The reflections at 38° and 44° correspond to metallic silver. The particle sizes calculated from the Figure 2(d) are 52.3, 51.6, and 53 nm for the blends (PS : P4VP) 75 : 25, 50 : 50, and 25 : 75, respectively, for the diffraction angle 38° . Electrical properties of polymer/metal composite films are strongly linked to particles' nanostructure.⁶ As the fraction of the metal in a nanocomposite increases the nanoparticle separation decreases resulted in better electrical properties of nanocomposites.²⁹ Therefore, electrical behavior of silver particulate films on PS/P4VP (50 : 50, 50 nm and 95 nm; 75 : 25, 50 nm and 150 nm) observed decrease in electrical resistance on increasing the thickness of films.¹⁹ Thus, electrical studies of these blends suggest possibility

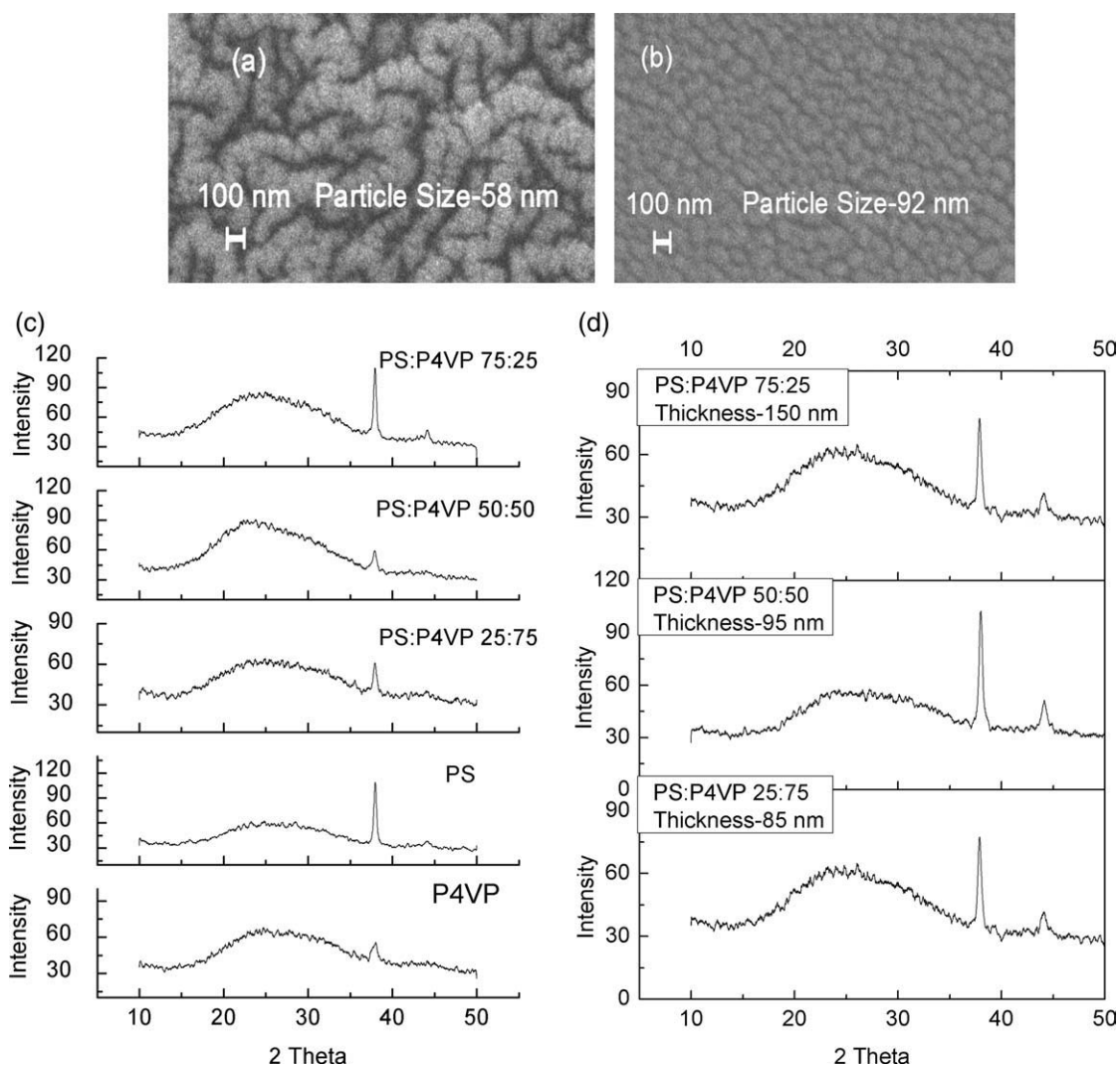


Figure 2 SEM images of PS/P4VP. (a) 0 : 100 and (b) 100 : 0 for silver particulate films of thickness 50 nm. Acceleration voltage-20 kV, Magnification 50 KX. (c) XRD curves for silver particulate films of thickness 50 nm on P4VP, PS, PS/P4VP, 25 : 75, 50 : 50, 75 : 25, respectively. (d) XRD curves for silver particulate films on PS/P4VP, 75 : 25, 50 : 50, and 25 : 75 for 150, 95, and 85 nm thicknesses.

of modification in morphology of silver particulate films on PS/P4VP as compared with films on PS.

Figure 1(b) shows the optical spectra recorded for the films of various thicknesses on PS/P4VP blends. The blend 50 : 50 shows the most promising result among all the silver particulate films on the blends. The intensity and shift of absorption peak is optimum (793 nm) for 95 nm film on PS/P4VP, 50 : 50. The silver particulate film of thickness 150 nm on PS/P4VP, 75 : 25 also shows a red shift (705 nm). This shift in the plasmon resonance peak towards higher wavelength can be attributed to close proximity of the silver clusters,²⁰⁻²³ perhaps this is the reason for the better electrical behavior of the film of thickness 150 nm on PS/P4VP, 75 : 25.¹⁹

Figure 1(c) shows the optical spectra for films of varying thickness on PS/P4VP, 50 : 50. The shift in plasma resonance towards higher wavelength indi-

cates close proximity of silver nanoparticles with increasing thickness of silver particulate films.⁸

Figure 1(d) shows the optical absorption spectra recorded for silver films on PS/P4VP, 75 : 25. It is clear that shift in surface plasma resonance is due to increase in particle size with the amount of silver deposited.⁸ The results are in agreement with the electrical properties of this blend which show increase in electrical conductivity on increasing silver loading.¹⁹

Micro structural studies

SEM of the silver particulate films [Fig. 2(a,b)] on homopolymers (PS, P4VP) clearly shows the characteristic nature of these polymers. The size and inter-separation of silver clusters is less (average particle size-58 nm) in P4VP whereas size as well as

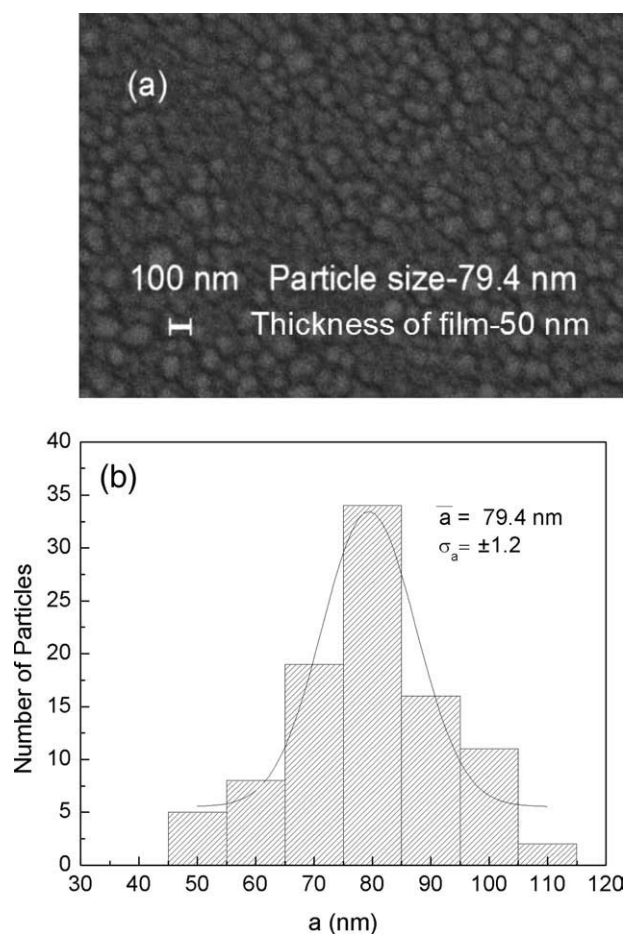


Figure 3 (a) SEM micrograph, Acceleration voltage-20 kV, Magnification 50 KX and (b) corresponding histogram of 50 nm thick silver film on PS/P4VP, 50 : 50.

interseparation is wide in PS (average particle size-92 nm). As a result, PS does not show the desired electrical conductivity.²⁶ Blending of P4VP into PS modifies size, size distribution, and interseparation of silver particles deposited on their blends PS/P4VP, 50 : 50, and 75 : 25. Figures 3(a)–6(a) show the SEM pictures of various thicknesses of silver films deposited on PS/P4VP blends. The acceleration voltage is 20 kV and magnification is 50–100 KX for all the SEM pictures. The particle sizes measured from respective SEM pictures are plotted as histogram in Figures 3(b)–6(b). The corresponding histograms [Figs. 3(b)–6(b)] of silver particles of the films are shown side by side of the SEM pictures. The data fit into a log normal distribution for all the cases. Hence, the average size, a and geometric standard deviation, σ_a are determined from the log normal distribution of the curves. The positive effect of blending P4VP with PS is clearly visible in these pictures. Figures 3(a) and 4(a) show the particle size distribution for 50 and 95 nm thick silver films deposited on PS/P4VP, 50 : 50. The average size, a and geometric standard deviation, σ_a are 79.4 nm and ± 1.2 , respectively, for

the 50 nm film whereas the corresponding values for the 95 nm film are 95.4 nm and ± 1.4 . A closer look at the morphology of silver nanoparticles deposited on PS/P4VP, 50 : 50 in Figures 3(a) and 4(a), clearly shows that particle size increases with the amount of silver deposited. The shape of the nanoparticles changes from near spherical particles to irregular ellipsoidal particles. The size distribution and width of histograms as shown in the figure indicate that the average size of the particle increases from 79.4 to 95.4 nm and the size distribution expands from 50 to 110 nm to 60–160 nm which results in improvement of tunneling effect in PS/P4VP, 50 : 50.¹⁹ And silver particulate film of thickness 95 nm show better electrical behavior than silver particulate film of 50 nm on PS/P4VP, 50 : 50.¹⁹ It is evident that increase in size distribution decreases the interseparation of silver clusters in this blend. This fact may be regarded as a consequence of the size as well as interseparation evolution of nanoparticles during the ongoing deposition process.

Figures 5(a) and 6(a) show the particle size distribution for 50 nm and 150 nm thickness films

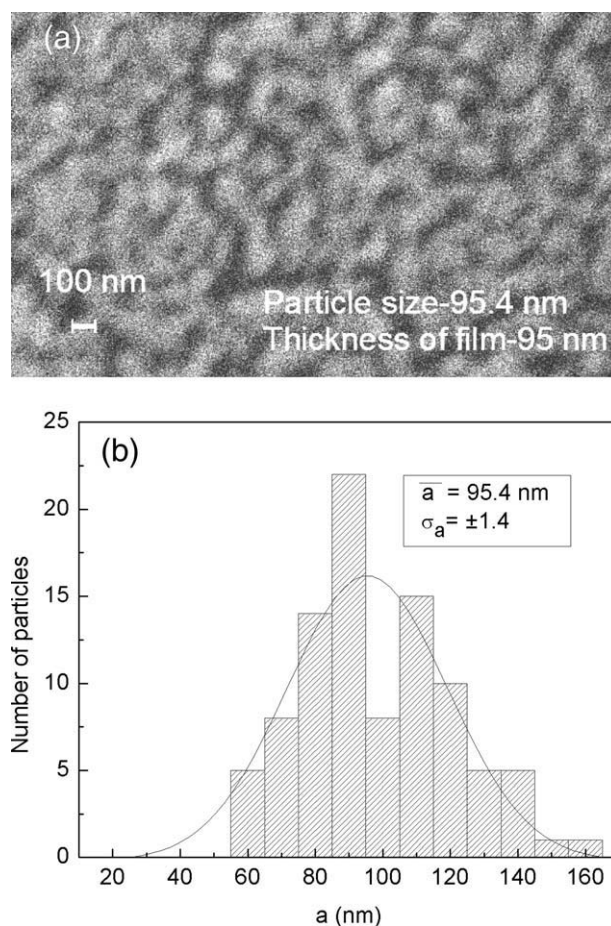


Figure 4 (a) SEM micrograph, Acceleration voltage-20 kV, Magnification 100 KX and (b) corresponding histogram of 95 nm thick silver film on PS/P4VP, 50 : 50.

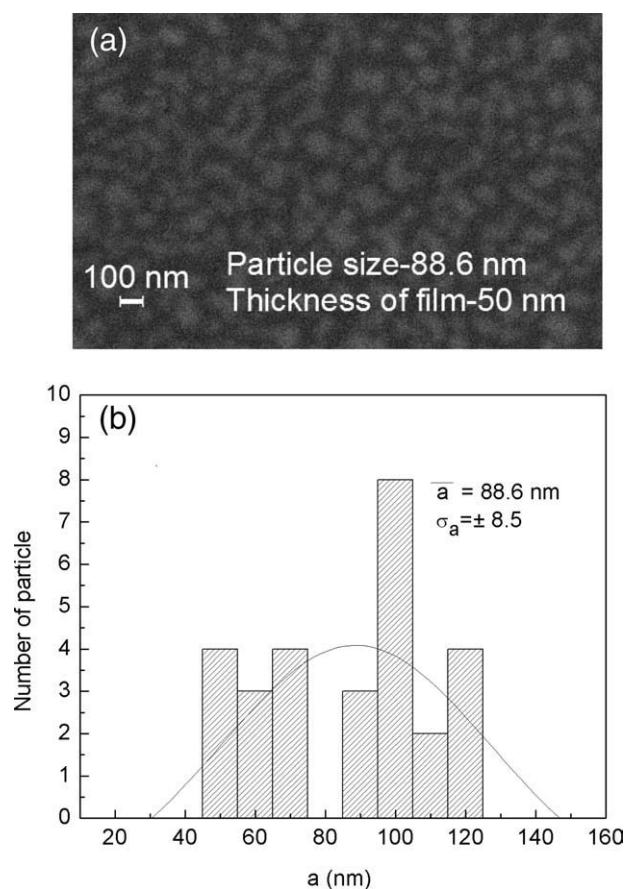


Figure 5 (a) SEM micrograph, Acceleration voltage-20 kV, Magnification 100 KX and (b) corresponding histogram of 50 nm thick silver film on PS/P4VP, 75 : 25.

deposited on PS/P4VP, 75 : 25. The average size, a and geometric standard deviation, σ_a are 88.6 nm and ± 8.5 for the 50 nm film and 96.7 nm and ± 4 for 150 nm film, respectively. It is evident from the figure that distribution of size increased from 50 to 120 nm to 60–140 nm. Such dispersion of silver nanoparticle within the PS/P4VP, 75 : 25 leads to better electrical behavior.¹⁹ Such electric behavior is not observed even for 300 nm silver particulate film on PS.²⁷ Hence, silver particulate film of 50 nm thickness on PS/P4VP, 75/25 consist of isolated and widely dispersed nanoparticles. But systematic and controlled increase of silver in the PS/P4VP, 75 : 25 matrices produced interesting result.¹⁹ The silver particulate film of thickness 150 nm on PS/P4VP, 75 : 25 shows the room temperature resistance in few mega ohms a desirable range for applications.

Table I has been compiled to show all the particles size of silver clusters embedded in PS/P4VP blends from XRD and SEM. The SEM has provided the morphology of silver clusters and their distribution. The XRD diffraction pattern represents the average throughout the film due to increased penetration and large beam size. The observed values of particle

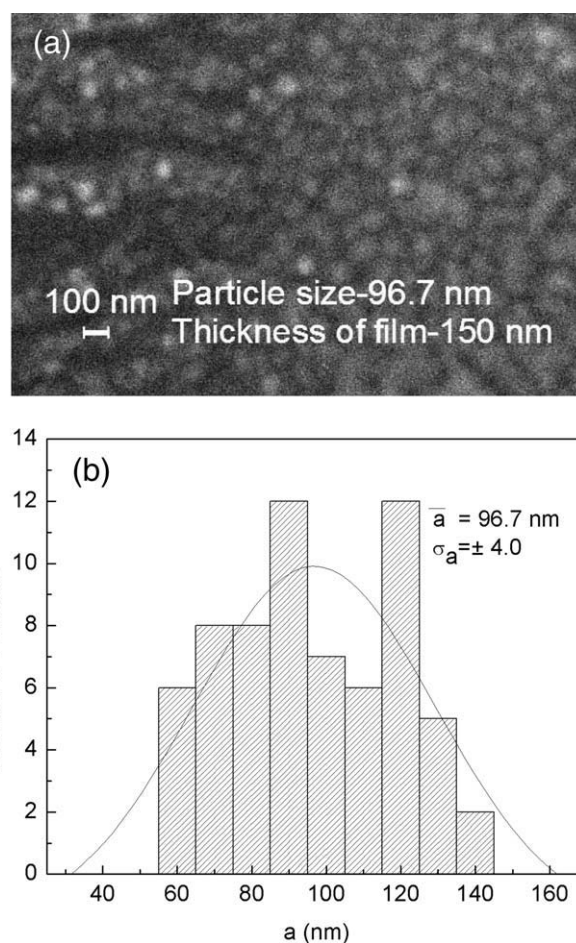


Figure 6 (a) SEM micrograph, Acceleration voltage-20 kV, Magnification 100 KX and (b) corresponding histogram of 150 nm thick silver film on PS/P4VP, 75 : 25.

size from SEM are in the same range as the calculated values of the particle size from XRD. The difference in the values may be due to averaging over longer depths because of penetration of X-rays. Although, the trend of particle size measured from XRD and SEM are similar.

TABLE I
The Average Particle Size for Silver Deposited on PS/P4VP Blends

PS/P4VP	Thickness (nm)	Particle size (nm)		Standard deviation σ_a
		XRD	SEM, a	
0 : 100	50	30	58	–
	25 : 75	46.6	–	–
50 : 50	85	53	–	–
	50	49.1	79.4	1.2
75 : 25	95	51.6	95.4	1.4
	50	51.8	88.6	8.5
100 : 0	150	52.3	96.7	4.0
	50	53.3	92	–

The deposition rate is 0.4 nm/s and temperature is 457 K.

CONCLUSIONS

The deposition of silver particulate films by evaporation on PS/P4VP blends yields positive effect of blending PS with P4VP. The size distribution and dispersion of silver nanoparticles is found to be dependent on the nature of the polymer host and thickness of particulate films. With the addition of P4VP and amount of silver, morphology of the silver particulate films on PS/P4VP (50 : 50, 75 : 25) could be modified to give the desired electrical results.

The author thanks DST for the XRD and NCL (Pune) for SEM facility.

References

1. Kunz, M. S.; Shull, K. R.; Kellock, A. J. *J Appl Phys* 1992, 72, 4458.
2. Korchev, A. S.; Bozack, M. J.; Slaten, B. L.; Mills, G. J. *Am Chem Soc* 2004, 126, 10.
3. Temgire, M. K.; Joshi, S. S.; *Rad Phys Chem* 2004, 71, 1039.
4. Inouye, H.; Tanaka, K.; Tanahashi, I.; Hattori, T. *Nakatsuka Jpn J Appl Phys* 2000, 39, 132.
5. Lin, J. C.; Wang, C. Y. *Mater Chem Phys* 1996, 45, 136.
6. Kiesow, A.; Morris, J. E.; Radehaus, C.; Heilmann, A. *J Appl Phy* 2003, 94, 10, 6988.
7. Kreibig, U.; Volmer, M. *Optical Properties of Metal Clusters*; Toennies, J. P., Ed.; Berlin: Springer, 1995.
8. Wang, X.; Zuo, J.; Keil, P.; Grundmeier, G. *Nanotechnology* 2007, 18, 265303.
9. Heilmann, A. *Polymer Films with Embedded Metal Nanoparticles*; Berlin: Springer, 2002.
10. Mayer, A. B. R. *Polym Adv Technol* 2001, 12, 96.
11. Beecroft, L. I. *Chem Mater* 1997, 9, 1302.
12. Caseri, W. *Macromol Rapid Commun* 2000, 21, 705.
13. Eilers, H.; Biswas, A.; Pounds, T. D.; Norton, M. G. *J Mater Res* 2006, 21, 2168.
14. Yonzon, C. R.; Stuart, D. A.; Zhang, X.; Mcfarland, A. D.; Haynes, C. L.; Duyne, R. P. V. *Talanta* 2005, 67, 438.
15. Pennelli, G. *Appl Phys Lett* 2006, 89, 163513.
16. Pattabi, M.; Rao, K. M.; Sainkar, S. R.; Sastry, M. *Thin Solid Films* 1999, 338, 40.
17. Rao, K. M.; Pattabi, M. J. *New Mat Electrochem Systems* 2001, 4, 11.
18. Hassell, T.; Yoda, S.; Howdle, S. M.; Brown, P. D. *J Phys Conf Series* 2006, 26, 276.
19. Parashar, P.; Pattabi, M.; Gurumurthy, S. C. *J Mater Sci Mater Electron* 2009, 20, 1182.
20. Heilmann, A.; Kiesov, A.; Gruner, M.; Kreibig, U. *Thin Solid Films* 1999, 343–344, 175.
21. Fritzsche, W.; Porwol, H.; Wiegand, A.; Boronmann; Khler, J. M. *Nanostrutured Mater* 1998, 10, 89.
22. Akamatsu, K.; Takei, S.; Mizuhata, M.; Kajinami, A.; Deki, S.; Fujii, M.; Hayashi, S.; Yamamoto, K. *Thin Solid Films* 2000, 359, 55.
23. Carotenuto, G. *Appl Organometal Chem* 2001, 15, 344.
24. Kim, J. Y.; Shin, D. H.; Ihn, K. J.; Suh, K. D. *J Ind Eng Chem* 2003, 9, 1, 37.
25. Heilmann, A.; Quinten, M.; Werner, J. *EurPhys JB* 1998, 3, 455.
26. Takele, H.; Greve, H.; Pochstein Zaporojtchenko, V.; Faupel, F. *Nanotechnology* 2006, 17, 3499.
27. Rao, K. M.; Pattabi, M.; Sainkar, S. R.; Mayya, K. S.; Sastry, M. *Thin Solid Films* 1997, 310, 97.
28. Rao, K. M.; Pattabi, M.; Sainkar, S. R.; Lobo, A.; Kulkarni, S. K.; Uchil, J.; Sastry, M. S. *J Phys D Appl Phys* 1999, 32, 2327.
29. Biswas, A.; Bayer Marken, I. S.; Pounds, T. D.; Norton, M. G. *Nanotechnology* 2007, 18, 305602.